The Design and Simulation of the Synthesis of Dimethyl Carbonate and the Product Separation Process Plant

Feng Wang[1], Ning Zhao[1], Fukui Xiao[1], Wei Wei[1] and Yuhan Sun[1,2]
*[1]State Key Laboratory of Coal Conversion, Institute of Coal Chemistry,
Chinese Academy of Sciences, Taiyuan Shanxi
[2]Low Carbon Energy Conversion Center, Shanghai Advanced Research Institute,
Chinese Academy of Sciences, Shanghai
P.R. China*

1. Introduction

Dimethyl carbonate (DMC) has become a green and environmental benign chemical due to its multiple reactivity and widely potential usage in chemical industry[1]. It has been used as a substitute to replace dimethyl sulfate and methyl halides in methylation reactions and as a carbonylation agent to substitute phosgene for the production of polycarbonates and urethane polymers. It also has been evaluated to apply as non-aqueous electrolyte component in lithium rechargeable batteries. Additionally, DMC is a strong contender to help the refining industry meet the Clean Air Act specifications for oxygen in gasoline. DMC has about 3 times the oxygen content as methyl tert-butyl ether (MTBE) and its synthesis is not dependent upon FCU isobutylene yields like MTBE. DMC has a good blending octane (R + M/2 = 105), it does not phase separate in a water stream like some alcohols do, and it is both low in toxicity and quickly biodegradable[2].

Many of the properties of DMC make it a genuinely green reagent, particularly if compared to conventional alkylating agents, such as methyl halides (CH_3X) and dimethyl sulfate (DMS) or to phosgene used as a methoxycarbonylating reagent. Firstly, DMC has been proved to be a nontoxic compound. Some of the toxicological properties of DMC and phosgene and DMS are compared in Table 1. Secondly, it has been classified as a flammable liquid, smells like methanol, and does not have irritating or mutagenic effects either by contact or inhalation. Therefore, it can be handled safely without the special precautions required for the poisonous and mutagenic methyl halides and DMS and the extremely toxic phosgene. Some physicochemical properties of DMC are listed in Table 2.

The phosgene-free route for synthesis of DMC has been widely concerned by academic and industrial researchers, such as the oxidative carbonylation of methanol, the transesterification of propylene or ethylene carbonate (PC or EC), the methanolysis of urea and direct synthesis of carbon dioxide with methanol. Recently, the newly derived route of the synthesis of DMC by urea methanolysis method was considered as a novel routine for the DMC synthesis because of the advantages of easily obtained materials, moderate

property	DMC	phosgene	DMS
oral acute toxicity (rats)	LD50 13.8 g/kg		LD50 440 mg/kg
acute toxicity per contact (cavy)	LD50 > 2.5 g/kg		
acute toxicity per inhalation (rats)	LC50 140 mg/L; (4 h)	LC50 16 mg/m3; (75 min)	LC50 1.5 mg/L (4 h)
mutagenic properties	none		mutagenic
irritating properties (rabbits, eyes, skin)	none	corrosive	
biodegradability (OECD 301 C)	> 90%(28 days)	rapid hydrolysis	rapid hydrolysis
acute toxicity (fish) (OECD 203)	NOEC[a] 1000 mg/L		LC50 10-100 mg/L (96 h)
acute toxicity on aerobial bacteria of wastewaters (OECD 209)	EC50 > 1000 mg/L		

[a] NOEC=Concentration which does not produce any effect.

Table 1. Comparison between the Toxicological and Ecotoxicological Properties of DMC, Phosgene, and DMS[1]

mp (°C)	4.6
bp (°C)	90.3
density (D^{20}_4)	1.07
viscosity (μ^{20}, cps)	0.625
flashing point (°C)	21.7
dielectric constant (ε^{25})	3.087
dipole moment (μ, D)	0.91
ΔH^{vap} (kcal/kg)	88.2
solubility H2O (g/100 g)	13.9
azeotropical mixtures	with water, alcohols, hydrocarbons

Table 2. Some Physical and Thermodynamic Properties of DMC[1]

reaction conditions and low investment for equipment. As a result, the separation of the reacted mixture which contain an azeotropic mixture of DMC and methanol became very important for the production of DMC.

2. The properties of DMC

The vapor pressure data of DMC

The vapor pressure of DMC has been measured by Rodriguez[3]. The data of the experiment of DMC has been showed in table 3, which could be regressed by the extended Antoine equation.

T (K)	P⁰(kPa)	T (K)	P⁰(kPa)	T (K)	P⁰(kPa)
326.06	26.66	372.06	133.29	393.98	247.92
328.41	29.32	372.67	135.96	394.39	250.58
330.58	31.99	373.27	138.62	394.80	253.25
332.61	34.66	373.91	141.29	395.18	255.92
334.53	37.32	374.54	143.95	395.58	258.58
336.34	39.99	375.15	146.62	395.99	261.25
338.03	42.65	375.73	149.28	396.38	263.91
339.64	45.32	376.33	151.95	396.77	266.58
341.20	47.98	376.89	154.62	397.16	269.24
342.68	50.65	377.37	157.28	397.54	271.91
344.09	53.32	377.94	159.95	397.95	274.58
345.45	55.98	378.47	162.61	398.29	277.24
346.75	58.65	379.02	165.28	398.67	279.91
348.04	61.31	379.63	167.94	398.93	282.57
349.26	63.98	380.05	170.61	399.30	285.24
350.43	66.64	380.62	173.28	399.66	287.91
351.57	69.31	381.16	175.94	400.02	290.57
352.69	71.98	381.71	178.61	400.38	293.24
353.77	74.64	382.23	181.27	400.66	295.90
354.81	77.31	382.71	183.94	400.99	298.57
355.86	79.97	383.22	186.61	401.35	301.23
356.85	82.64	383.73	189.27	401.66	303.90
357.81	85.31	384.40	191.94	402.03	306.57
358.72	87.97	384.98	194.60	402.39	309.23
359.63	90.64	385.48	197.27	402.76	311.90
360.54	93.30	385.95	199.93	403.11	314.56
361.73	95.97	386.45	202.60	403.46	317.23
362.14	97.30	386.92	205.27	403.80	319.89
362.55	98.63	387.40	207.93	404.50	325.23
362.98	99.97	387.91	210.60	405.15	330.56
363.46	101.30	388.33	213.26	405.45	333.22
363.84	102.63	388.77	215.93	406.12	338.56
364.24	103.97	389.25	218.59	406.75	343.89
364.65	105.30	389.70	221.26	407.03	346.55
365.04	106.63	390.14	223.93	407.69	351.88
365.63	109.30	390.59	226.59	408.31	357.22
366.37	111.96	391.04	229.26	408.56	359.88
367.10	114.63	391.45	231.92	409.22	365.21
367.89	117.29	391.89	234.59	409.82	370.54
368.65	119.96	391.89	234.59	410.13	373.21
369.38	122.63	392.31	237.26	410.71	378.54
370.10	125.29	392.75	239.92	411.09	381.21
370.80	127.96	393.15	242.59	411.29	383.87
371.47	130.62	393.55	245.25		

Table 3. Experimental vapor pressure and boiling point for DMC

3. The vapor-liquid equilibrium

Vapour–liquid equilibrium (VLE) data are always required for engineering, such as designing in distillation tower, which is the most common operation performed in the chemical industry for the separation of liquid mixture. Dimethyl carbonate and methanol constitute azeotropic mixture in a composition ratio of 30:70 (weight ratio), and thus it is difficult to separate the mixture by distillation under normal pressure. ENIChem has a German patent showing that the percentage of methanol in the binary methanol–DMC azeotrope increases with pressure: going from 70% methanol at 101.33 kPa, up to 95% methanol at 1013.3 kPa.

3.1 The VLE for methanol and DMC

The thermodynamic properties of the binary methanol (1)–DMC (2) under atmosphere pressure have been reported, as well as the relationship of temperature and the binary azeotrope. Zhang and Luo reported the only calculated the binary vapor liquid equilibrium (VLE) data under normal pressure based on group contribution UNIFAC method. Li et al. measured the related binary VLE data with an Ellis Cell at 101.325 kPa. Rodriguez et al. also measured the vapor–liquid equilibria of dimethyl carbonate with linear alcohols by a dynamic re-circulating method under normal pressure, and estimated the new interaction parameters for UNIFAC and ASOG method. Theoretically, the predictive group contribution methods may be applicable until 0.5MPa. Based on the above methods, both of the vapor and liquid phases were directly sampled and analyzed.

Vapour–liquid equilibrium data for methanol (1) +DMC (2) system at normal pressure has been presented in table coming from A. Rodriguez [4]. The results reported in these tables indicate that the binary systems of methanol – DMC exhibited a positive deviation from ideal behaviour and a minimum boiling azeotrope.

T (K)	x	y	γ_1	γ_2
361.99	0.0103	0.0523	2.219	0.993
359.93	0.0252	0.1258	2.326	0.992
357.45	0.0457	0.2065	2.280	0.996
355.71	0.0620	0.2669	2.298	0.992
354.69	0.0709	0.2950	2.297	0.996
352.38	0.0958	0.3613	2.249	1.002
349.83	0.1291	0.4379	2.204	0.999
347.97	0.1582	0.4818	2.110	1.017
346.56	0.1834	0.5202	2.064	1.021
344.85	0.2210	0.5687	1.989	1.023
343.99	0.2472	0.5915	1.906	1.035
342.57	0.2913	0.6238	1.795	1.067
341.74	0.3251	0.6488	1.724	1.079
340.99	0.3619	0.6703	1.644	1.102

T (K)	x	y	$\gamma 1$	$\gamma 2$
340.11	0.4247	0.6960	1.502	1.165
339.18	0.4916	0.7206	1.390	1.256
338.69	0.5386	0.7394	1.325	1.316
338.21	0.5800	0.7547	1.279	1.386
337.55	0.6622	0.7806	1.187	1.582
337.18	0.7181	0.7955	1.131	1.794
336.97	0.7684	0.8123	1.088	2.022
336.95	0.8160	0.8332	1.051	2.265
336.88	0.8617	0.8560	1.025	2.612
336.89	0.8824	0.8736	1.021	2.698
336.98	0.9104	0.8931	1.008	2.988
337.11	0.9341	0.9166	1.003	3.158
337.25	0.9549	0.9406	1.002	3.273
337.39	0.9726	0.9614	1.000	3.487
337.60	0.9889	0.9833	0.998	3.699

Table 4. Vapour–liquid equilibrium data for methanol (1) +DMC (2) system at 101.3 kPa[4]

The azeotrope data for methanol-DMC on the high pressure has been show on the following table, which was a comparison of the data from different literature. The data has exhibited the composition of DMC in an azeotrope of DMC-methanol decreased with the increases of pressure. These thermodynamic data showed that the separation of the mixture of methanol and DMC would be difficult with the normal distillation.

T (K)	p (kPa)	x1	w1	p(kPa)	x1	w1
337.35	102.73	0.8500	0.6684	101.33	0.8677	0.7000
377.15	405.70	0.9100	0.7824	405.2	0.9150	0.7929
391.15	613.00	0.9150	0.7929	607.8	0.9298	0.8249
411.15	1077.00	0.9200	0.8036	1013.0	0.9521	0.8761
428.15	1576.00	0.9625	0.9013	1519.5	0.9739	0.9300

Table 5. Comparisons of azeotrope data for methanol (1)–dimethyl carbonate (2) binary system at different temperatures from different literature.

3.2 The VLE for DMC with other compound

T (K)	x	y	$\gamma 1$	$\gamma 2$
362.37	0.0180	0.0494	1.853	0.992
361.70	0.0293	0.0790	1.864	0.993
361.00	0.0394	0.1044	1.877	0.997

T (K)	x	y	$\gamma 1$	$\gamma 2$
359.81	0.0591	0.1520	1.900	1.001
358.27	0.0882	0.2157	1.909	1.004
357.07	0.1128	0.2628	1.899	1.008
355.97	0.1386	0.3071	1.879	1.011
355.07	0.1621	0.3413	1.846	1.018
354.07	0.1906	0.3776	1.802	1.030
353.19	0.2193	0.4151	1.779	1.033
352.20	0.2564	0.4507	1.714	1.054
351.56	0.2871	0.4786	1.665	1.066
350.70	0.3352	0.5160	1.588	1.093
350.45	0.3539	0.5315	1.564	1.098
350.00	0.3902	0.5549	1.507	1.123
349.68	0.4141	0.5696	1.475	1.143
349.40	0.4504	0.5842	1.406	1.189
349.17	0.4832	0.6031	1.365	1.216
349.00	0.5097	0.6156	1.329	1.249
348.86	0.5383	0.6266	1.288	1.295
348.75	0.5671	0.6396	1.253	1.339
348.66	0.5945	0.6538	1.226	1.377
348.61	0.6125	0.6625	1.208	1.408
348.57	0.6330	0.6728	1.189	1.443
348.45	0.6721	0.6925	1.158	1.525
348.46	0.7173	0.7101	1.112	1.668
348.57	0.7481	0.7286	1.089	1.746
348.70	0.7824	0.7491	1.065	1.861
348.93	0.8297	0.7818	1.039	2.053
349.06	0.8472	0.7938	1.028	2.153
349.34	0.8740	0.8184	1.016	2.278
349.60	0.8976	0.8429	1.008	2.405
349.83	0.9166	0.8662	1.006	2.496
350.23	0.9417	0.8984	1.000	2.677
350.71	0.9667	0.9335	0.993	3.020
350.95	0.9775	0.9543	0.995	3.048
351.13	0.9875	0.9730	0.997	3.223

Table 6. Vapor–liquid equilibrium data for ethanol (1) + DMC (2) system at 101.3 kPa[4]

T (K)	x	y	$\gamma 1$	$\gamma 2$
369.72	0.0124	0.0356	2.368	0.998
369.19	0.0229	0.0622	2.275	1.000
368.66	0.0342	0.0894	2.223	1.002
368.20	0.0458	0.1165	2.193	1.001
367.51	0.0628	0.1543	2.161	1.001
366.86	0.0818	0.1872	2.052	1.006
366.21	0.1021	0.2217	1.985	1.009
365.43	0.1303	0.2596	1.865	1.021
365.05	0.1440	0.2801	1.841	1.024
364.49	0.1669	0.3089	1.782	1.031
364.05	0.1859	0.3308	1.736	1.040
363.37	0.2262	0.3695	1.627	1.058
362.96	0.2504	0.3922	1.580	1.070
362.59	0.2767	0.4120	1.519	1.088
362.31	0.2975	0.4317	1.493	1.095
361.89	0.3407	0.4596	1.406	1.127
361.49	0.3796	0.4855	1.349	1.159
361.31	0.4089	0.5057	1.312	1.177
361.12	0.4365	0.5232	1.279	1.200
360.94	0.4721	0.5424	1.233	1.238
360.70	0.5064	0.5620	1.200	1.280
360.59	0.5363	0.5790	1.171	1.315
360.49	0.5616	0.5931	1.149	1.350
360.35	0.5916	0.6101	1.127	1.396
360.30	0.6213	0.6279	1.106	1.440
360.27	0.6558	0.6473	1.081	1.504
360.20	0.6846	0.6682	1.071	1.549
360.25	0.7185	0.6900	1.052	1.618
360.31	0.7524	0.7142	1.038	1.693
360.55	0.7885	0.7458	1.026	1.746
360.82	0.8269	0.7793	1.014	1.834
361.07	0.8643	0.8163	1.008	1.929
361.31	0.8840	0.8380	1.004	1.972
361.78	0.9163	0.8738	0.995	2.091
362.34	0.9494	0.9168	0.990	2.232
362.99	0.9774	0.9613	0.989	2.268

Table 7. Vapor–liquid equilibrium data for DMC (1) + 1-propanol (2) system at 101.3 kPa[4]

T (K)	x	y	$\gamma 1$	$\gamma 2$
389.73	0.0120	0.0582	2.314	0.992
387.85	0.0315	0.1389	2.207	0.987
386.14	0.0490	0.1985	2.118	0.994
384.59	0.0678	0.2563	2.058	0.994
383.07	0.0862	0.3072	2.019	0.998
381.06	0.1158	0.3785	1.954	0.996
379.14	0.1454	0.4314	1.868	1.013
377.02	0.1845	0.4946	1.789	1.022
374.93	0.2287	0.5499	1.701	1.043
373.03	0.2797	0.5976	1.596	1.075
371.60	0.3265	0.6355	1.514	1.103
370.59	0.3654	0.6617	1.451	1.131
370.02	0.3897	0.6768	1.415	1.150
369.00	0.4397	0.7044	1.344	1.194
368.46	0.4694	0.7194	1.307	1.223
368.05	0.4941	0.7312	1.277	1.250
367.53	0.5268	0.7464	1.242	1.288
366.97	0.5638	0.7638	1.207	1.332
366.34	0.6087	0.7838	1.169	1.396
365.81	0.6478	0.8021	1.142	1.451
365.12	0.7029	0.8218	1.101	1.595
364.41	0.7646	0.8492	1.069	1.756
363.89	0.8175	0.8677	1.038	2.032
363.63	0.8497	0.8829	1.024	2.209
363.49	0.8911	0.9008	1.001	2.600
363.31	0.9335	0.9328	0.995	2.910
363.28	0.9678	0.9662	0.995	3.030

Table 8. Vapor–liquid equilibrium data for DMC(1) + 1-butanol (2) system at 101.3 kPa[4]

T (K)	x	y	$\gamma 1$	$\gamma 2$
409.75	0.0082	0.0469	1.687	1.006
408.28	0.0180	0.0970	1.642	1.009
405.75	0.0373	0.1863	1.611	1.008
403.40	0.0557	0.2587	1.581	1.013
400.41	0.0824	0.3516	1.558	1.010
397.81	0.1081	0.4229	1.520	1.013
393.86	0.1493	0.5209	1.492	1.016

T (K)	x	y	$\gamma 1$	$\gamma 2$
390.21	0.1955	0.6031	1.446	1.018
386.97	0.2443	0.6677	1.392	1.025
384.83	0.2811	0.7065	1.354	1.034
383.23	0.3127	0.7340	1.319	1.043
381.83	0.3431	0.7573	1.288	1.053
380.09	0.3845	0.7843	1.247	1.071
378.47	0.4274	0.8095	1.211	1.086
376.75	0.4790	0.8336	1.167	1.119
375.97	0.5027	0.8437	1.150	1.138
374.58	0.5509	0.8615	1.115	1.183
373.25	0.5998	0.8786	1.085	1.232
371.89	0.6466	0.8945	1.065	1.285
370.46	0.6979	0.9115	1.049	1.341
369.29	0.7370	0.9244	1.042	1.386
368.36	0.7775	0.9345	1.027	1.479
366.72	0.8413	0.9530	1.016	1.601
365.10	0.9063	0.9724	1.011	1.713
364.64	0.9371	0.9814	1.001	1.757
363.96	0.9693	0.9904	0.997	1.917

Table 9. Vapor–liquid equilibrium data for DMC(1) + 1-pentanol (2) system at 101.3 kPa[4]

The azeotropic mixture of DMC with some common compounds has been listed in table 10[4].

Component	T(K)	Composition (mol%)
Methanol	336.90	0.8503
Ethanol	348.46	0.7055
1-propanol	360.29	0.6364
1-butanol	363.32	0.9306

Table 10. the azeotropic mixtures of DMC with some compounds at 101.3 kPa

4. The calculation of VLE

Rigorous thermodynamic model is the base of the process simulation and optimization. The vapor–liquid equilibrium relations for a binary system are:

$$\hat{f}_i^G(T,p,y_i,k_{i,i}) = \hat{f}_i^L(T,p,x_i,k_{i,j})$$

These correlations could be resolved by the Equation of State (EOS) functions. Although, Shi has correlated the vapor liquid equilibrium of methanol and DMC from the experiment data

by a modified Peng-Robinson equation of stage both for the liquid and vapor phase, there had none of the EOS now available can simultaneously describe both of the liquid and vapor phase thermo-dynamical properties accurately, especially for liquid or liquid mixtures. Although EOS well expresses the p–V–T relationship of vapor or gas phase, the calculation for liquid density now is an unsubstantial domain for EOS. That is said that we cannot directly use EOS to predict the molar volume and fugacity of a liquid phase accurately.

Nowadays, the commonly used for the calculation of vapor liquid equilibrium was the combination of EOS + γ method, which the EOS computed for the vapor phase and γ for the liquid phase. And also the Henry's method was used to describe the gas liquid equilibrium.

Here listed one of EOS for the vapor or gas phase. The Peng-Robinson equation of state can be used to evaluate the compressibility factor and species fugacity coefficient.

$$P = \frac{RT}{v-b} - \frac{a}{V(V+b)+b(V-b)}$$

$$a = 0.45724\alpha(T_r)R^2Tc^2 / Pc$$

$$b = 0.077880RTc / Pc$$

Shi et al used the follow correlation for the calculation of parameters of methanol and DMC:

$$\alpha(T_r) = 1 + (1-T_r)\left(m + n/T_r^2\right)$$

The parameter of m and n for methanol and DMC was show below.

Methanol: m 1.1930; n 0.09370

DMC: m 1.0236; n 0.06463

The parameter also can be estimated by the following correlation:

$$\alpha(T_r,\omega) = \left[1 + \left(0.37464 + 1.54226\omega - 0.26992\omega^2\right)\left(1 - T_r^{1/2}\right)\right]^2 ; \ 0 < \omega < 0.5$$

$$\alpha(T_r,\omega) = \left[1 + \left(0.3796 + 1.4850\omega - 0.1644\omega^2 + 0.0166\omega^3\right)\left(1 - T_r^{1/2}\right)\right]^2 ; \ 0.2 < \omega < 2.0$$

For the $0.2 < \omega < 0.5$, the function get the similar estimated value.

The mixing rule for the function used is as follow:

$$b = \sum x_i b_i$$

$$a = \sum\sum x_i x_j a_{i,j}$$

$$a_{i,j} = a_i^{1/2} a_j^{1/2}(1-k_{ij})$$

The Peng-Robinson equation of state may be written in compressibility factor form:

$$Z^3 - (1-B)Z^2 + (A - 2B - 3B^2)Z - (AB - B^2 - B^3) = 0$$

$$A = ap/(RT)^2, \ B = bp/(RT)$$

φ_i^G is expressed as follow:

$$\ln \varphi_i^G = Z_i - 1 - \ln(Z_i - \beta_i) - q_i I_i$$

where Z_i is the compressibility factor and obtained from Eq. (4);

$$\beta = \Omega P_r / T_r \ ; \ q = \Psi \alpha(T_r) P_r / (\Omega T_r); \ I = \frac{1}{\sigma - \varepsilon} \ln\left(\frac{Z + \sigma\beta}{Z + \varepsilon\beta}\right)$$

EoS	$\alpha(T_r)$	σ	ε
PR	$\alpha(T_r, \omega)^a$	$1 + \sqrt{2}$	$1 - \sqrt{2}$

a $\alpha(T_r, \omega) = \left[1 + \left(0.37464 + 1.54226\omega - 0.26992\omega^2\right)\left(1 - T_r^{1/2}\right)\right]^2$

Table 11. Parameter assignments for PR EoS[5].

Substance	Tc/K	pc/MPa	ω
CO	132.85	3.494	0.045
O2	154.58	5.043	0.022
CO2	304.12	7.374	0.225

Table 12. Critical constants and acentric factors[5]

1. the method for the liquid activity coefficient
   a. the Wilson method

$$\ln \gamma_i = 1 - \ln \sum_j x_j \Lambda_{ij} - \sum_j (x_j \Lambda_{ji} / \sum_l x_l \Lambda_{jl})$$

where: $\Lambda_{ii} = 1$

$$\Lambda_{ij} = \left(\frac{V_j^L}{V_i^L}\right) \exp\left(-\frac{\lambda_{ij} - \lambda_{ii}}{RT}\right)$$

Where V represents the liquid molar volume of pure component; $\lambda_{ij} - \lambda_{ij}$ represents the energy parameter.

The Wilson model is not supported for the prediction of the liquid-liquid equilibria.

b.   the NRTL method

The non-random two-liquid model (NRTL equation) is an activity coefficient model that correlates the activity coefficients γ_i of a compound i with its mole fractions xi in the liquid phase concerned. The concept of NRTL is based on the hypothesis of Wilson that the local concentration around a molecule is different from the bulk concentration. This difference is due to a difference between the interaction energy of the central molecule with the molecules of its own kind U_{ii} and that with the molecules of the other kind U_{ij}. The energy difference also introduces a non-randomness at the local molecular level.

The general equation is:

$$\ln(\gamma_i) = \frac{\sum_{j=1}^{n} x_j \tau_{ji} G_{ji}}{\sum_{k=1}^{n} x_k G_{ki}} + \sum_{j=1}^{n} \frac{x_j G_{ij}}{\sum_{k=1}^{n} x_k G_{kj}} \left(\tau_{ij} - \frac{\sum_{m=1}^{n} x_m \tau_{mi} G_{mi}}{\sum_{k=1}^{n} x_k G_{kj}} \right)$$

with

$$G_{ij} = \exp(-\alpha_{ij} \tau_{ij})$$

$$\alpha_{ij} = \alpha_{ij0} + \alpha_{ij1} T$$

$$\tau_{ij} = A_{ij} + \frac{B_{ij}}{T} + \frac{C_{ij}}{T^2} + D_{ij} \ln(T) + E_{ij} T^{F_{ij}}$$

c.   the UNIFAC method

The UNIversal Functional Activity Coefficient (UNIFAC) method is a semi-empirical system for the prediction of non-electrolyte activity estimation in non-ideal mixtures, which was first published in 1975 by Fredenslund, Jones and Prausnitz. UNIFAC uses the functional groups present on the molecules that make up the liquid mixture to calculate activity coefficients. By utilizing interactions for each of the functional groups present on the molecules, as well as some binary interaction coefficients, the activity of each of the solutions can be calculated.

In the UNIFAC model the activity coefficients of component i of a mixture are described by a combinatorial and a residual contribution.

$$\ln \gamma_i = \ln \gamma_i^C + \ln \gamma_i^R$$

Combinatorial part

$$\ln \gamma_i^C = \ln \frac{J_i}{x_i} + 1 - \frac{J_i}{x_i} - \frac{1}{2} Z q_i \left(\ln \frac{\varphi_i}{\theta_i} + 1 - \frac{\varphi_i}{\theta_i} \right)$$

where $J_i = x_i r_i^{2/3} / \sum x_j r_j^{2/3}$; $\varphi_i = x_i r_i / \sum x_j r_j$; $\theta_i = x_i q_i / \sum x_j q_j$ and Z = 10.

The coordination number, z, i.e. the number of close interacting molecules around a central molecule, is frequently set to 10. It can be regarded as an average value that lies between cubic (z=6) and hexagonal packing (z=12) of molecules that are simplified by spheres.

Where r_i is the volume parameters of component i, computed by $r_i = \sum v_j^{(i)} R_j$. Where the $v_j^{(i)}$ is the number of groups of type k in component i, and R_j is the volume parameter for group k; q_i is the area parameter for component i, calculated as $q_i = \sum v_j^{(i)} Q_j$.

Residual part

$$\ln \gamma_i^R = \sum_k v_k^{(i)} \left(\ln \Gamma_k - \ln \Gamma_k^{(i)} \right)$$

k is the group activity coefficient of group k in the mixture and (i) k is the group activity coefficient of group k in the pure substance.

$$\ln \Gamma_k = Q_k \left[1 - \ln \left(\sum_m \theta_m \tau_{mk} \right) - \sum_m \frac{\theta_m \tau_{mk}}{\sum_n \theta_n \tau_{nk}} \right]$$

$$\theta_m = \frac{Q_m X_m}{\sum Q_n X_n} ; \ X_m = \frac{\sum_j v_m^{(j)} x_j}{\sum_j \sum_n v_n^{(j)} x_j}$$

X_m represents the fraction of group m in the mixture.

$$\tau_{nm} = \exp \left(\frac{-(u_{nm} - u_{mm})}{T} \right)$$

Where the energy parameter of u_{ij} characterize the interaction between group i and j, and estimated from experiment data.

Alternatively, in some process simulation software τ_{ij} can be expressed as follows:

$$\ln \tau_{ij} = A_{ij} + B_{ij} / T + C_{ij} \ln T + D_{ij} T^2 + E_{ij} / T^2$$

The "C", "D", and "E" coefficients are primarily used in fitting liquid–liquid equilibria (with "D" and "E" rarely used at that). The "C" coefficient is useful in vapor-liquid equilibria as well.

For the system mixture of DMC-Phenol and Phenol-Methanol

Wang[6] measured the DMC-Phenol and Phenol-Methanol mixture system and predicted the VLE by the Wilson, NRTL, UNIQUAC equations with considering the ideal vapor behavior. The Wilson, NRTL, UNIQUAC equations energy

parameters can be obtained using the following expressions where a_{ij} , b_{ij} are the binary parameters regressed.

Wilson: $\Lambda_{ij} = \exp(a_{ij} + b_{ij} / T)$

NRTL: $\tau_{ij} = a_{ij} + b_{ij} / T$

UNIQUAC: $\tau_{ij} = \exp(a_{ij} + b_{ij} / T)$

The regressed parameter from the experiment obtained by Wang listed in table 13.

equation	parameters	Phenol(1)-DMC(2)	Phenol(1)-methanol(2)
Wilson	a_{12}; b_{12}	-3.215767; 1465.520	-4632.789; 9.657878
	a_{21}; b_{21}	1.213508; -423.7649	1777.066; -3.209978
NRTL	a_{12}; b_{12}	-0.9630158; 386.8243	1712.322; -5.054467
	a_{21}; b_{21}	3.061205; -1467.521	-3715.243; 9.690805
	α	0.300	0.300
UNIQUAC	a_{12}; b_{12}	0.7670656; -273.3901	-7802.509; -85.39368
	a_{21}; b_{21}	-1.505834; 691.9294	289.7973; 0.2346874

Table 13. Binary parameters of Wilson, NRTL and UNIQUAC equations

2. Calculating the fugacity of gas in liquid by Henry's method

For estimating the fugacity of component i in the liquid (L) phase, Eq. (6) was proposed by Sander et al.

$$\hat{f}_1^L = x_i H_{i,r} \gamma_i \big/ \gamma_{i,r}^\infty$$

where the subscript i and r represent a gas and a reference solvent, respectively. $H_{i,r}$ is Henry's constant for gas i in a reference solvent. γ_i is called the activity coefficient in the unsymmetric convention. $\gamma^\infty_{i,r}$ is the activity coefficient at infinite dilution in the symmetric convention.

The reference Henry's constant $H_{i,r}$ is calculated as a function of temperature from the following expression,

$$\ln\left(H_{i,r} / Pa\right) = \left(A + \frac{B}{T} + C \ln T \right) \times 101325$$

Wang et. al.[5] has studied the gas liquid equilibrium of CO, O2 and CO2 with DMC by the Henry method with the UNIFAC model for liquid system. Table 14 and 15 presents the chosen reference solvents for studied gases (CO, O_2 and CO_2) in the Wang's work and the estimated parameters A, B and C for calculating the reference Henry's constant. The activity coefficients i is obtained from the modified UNIFAC model. The UNIFAC energy parameter that was obtained by Wang has listed in Table 16. And also the parameter data can be obtained in Wang's article.

Gas	A	B	C	Reference solvent
CO	7.53116	-6.36893	0.0	Propanol
O2	26.1577	-924.307	-2.73771	Ethanol
CO2	27.5146	-1846.89	-2.99332	Hexadecane

Table 14. Constants for calculation of reference Henry's constant according to Henry constant equation.

Group	Rk	Qk
CO	2.094	2.120
O2	1.764	1.910
CO2	2.592	2.522
CH3	1.8022	1.696
CH2	1.3488	1.080
OH	1.060	1.168
–OCOO–	3.1642a	2.7874b

[a] R – OCOO – = 2[Van der Waal's volume from Bondi [20]]/15.17cm3 mol-1.
[b] Q – OCOO – = 2[Van der Waal's area from Bondi [20]]/(2.5x109) cm2 mol-1.

Table 15. The group parameters Rk and Qk values for GLE calculation.

Energy parameters, unm(K)	CO	O2	CO2	–CH3
–OCOO–	−364.4	−328.5	−4.4	−786.5

Table 16. The new UNIFAC interaction-energy parameters obtained by Wang

5. Model for catalytic distillation for the synthesis of DMC by urea and methanol

The current routes for the DMC synthesis are the oxy-carbonylation of methanol (EniChem process and UBE process) and the trans-esterification method (Texaco process). Recently, an attractive route for the synthesis of DMC by a urea methanolysis method over solid bases catalyst has been carried out in a catalytic distillation

The catalytic distillation (CD) [7], which is also known as reactive distillation (RD) that combines the heterogeneous catalyzed chemical reaction and the distillation in a single unit, has attracted more interest in academia and become more important in the chemical processing industry as it has been successfully used in several important industrial processes. The CD provides some advantages such as high conversion in excess of the chemical equilibrium, energy saving, overcoming of the azeotropic limitations and prolonging the catalyst lifetime.[8] The number of the contributions both for the simulative and experimental investigations about catalytic distillation are greatly increasing in recent years, especially for the modeling and simulation studies. And the applications of the

catalytic distillation in its field are expanding. The modeling analysis approach for the design, synthesis, and feasibility analysis of the reactive distillation process have been parally developed since the equilibrium stage model was used for process analysis through computer in late 1950s.

On current knowledge, the real distillation process always operates away from equilibrium and for multi-component mass transfer in the distillation, and the stage efficiency is often different for each component.[9] In recent years, the non-equilibrium model, also called rate-based model, has been developed for reactive distillation column to describe the mass transfer between vapor and liquid phase using the Maxwell-Stefan equations.[10] Always, the two phase non-equilibrium model is used for the prediction of the catalytic distillation, which treats the solid catalyst as a pseudo-liquid phase for the reaction in the catalyst. Also a more complex three-phase model [11] have been developed in some contributions in recent years to rigorously describe the reaction kinetics and mass transfer rate between the liquid and the solid catalytic phase in the catalytic distillation. However, a pseudo-homogeneous non-equilibrium model might adequately simulate the temperature profile, yield and selectivity for a CD process for a kinetically controlled reaction system. Additionally, the difficulties are related to the determination of additional model parameters required when using such models, and good estimation methods for the calculation of the diffusion coefficients and the non-ideal thermodynamic behavior inside a catalyst are also absent.

In our former work[12], modeling and simulation of such a catalytic distillation process for the DMC synthesis from urea and methanol was carried out based on the non-equilibrium model. The heterogeneously catalyzed reactions in the liquid bulk phase are considered as pseudo-homogeneous for the synthesis of DMC. Furthermore, the effect of distillation total pressure and the reaction temperature was studied. The interaction between the chemical reaction and the product separation were illustrated with the non-equilibrium model. And the mass transfer rate between the liquid and vapor phase have been taken into account by using the Maxwell-Stefan equations.

5.1 The configuration of the simulated catalytic distillation

The simulated column, a two meter tall stainless steel reactive distillation with an inner diameter of 22 mm, was configured with two feeding inlets and a side outlet. The materials were fed into the distillation column through preheater with volumes of 500ml for each feed stream. It would take about 2-5 hours for the feed material to pass though the preheater to the distillation column, which was enough for the complete conversion of urea to MC in the preheater, as the first reaction for DMC synthesis by urea methanolysis method could take place with high yield even in the absence of catalyst. The distillation column was divided into three sections, the rectifying section, the reaction section and the stripping section. 100 ml catalyst pellets weighted 103g with an average diameter of 3 mm were randomly packed in the reaction zone and the grid metal rings with a diameter of 3.2 mm were packed into the non-reaction zones. The distillation configured with a partial condenser to release the non-condensing gas of ammonia and a partial reboiler to discharge the heavy component of MC. The temperature in the reaction zone was set to 454.2 K for the synthesis reaction and the process was carried out under the pressure of 9-13 atm.
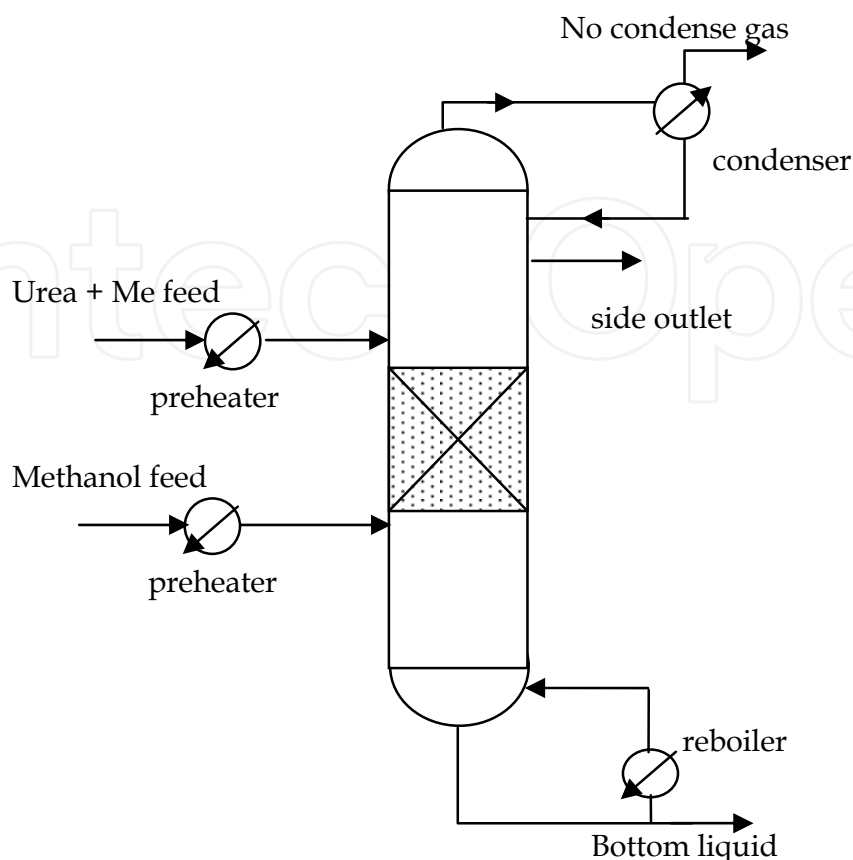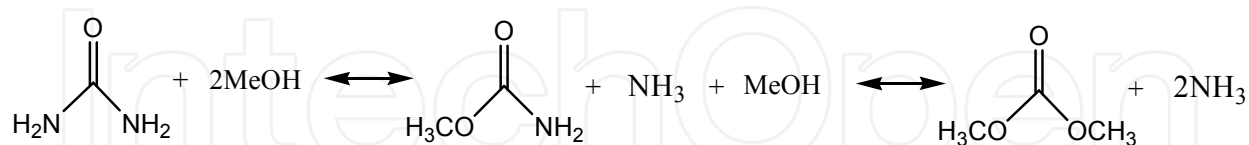
Fig. 1. The scheme of the catalytic distillation for synthesis of DMC

5.2 Chemical reactions

The synthesis of DMC from urea and methanol is catalyzed by the solid base catalysts shown in the scheme.

Scheme 1. the synthesis of DMC from Urea and methanol

The synthesis of DMC is a two-step reaction. The intermediate methyl carbamate (MC) is produced with high yield in the first step and further converted to DMC by reacting with methanol on catalyst in the second step. Our co-workers have developed the ZnO catalyst to catalyze the DMC synthesis reaction in CD process, which exhibited high activity toward the reactions. It was found by our workers that the reaction of the first step took place with high yield even in the absence of catalyst, and the catalyst was mainly effective for the second step. In CD process for the synthesis of DMC, the material mixture of urea and methanol was fed in the CD column through a preheater which has been heated to 423K and the materials stayed in the preheater for sufficient time to convert the urea to MC. As a

result, only second step of DMC synthesis reaction, where MC converting to DMC, took place in the catalytic distillation column (shown as follow).

$$MC + MeOH \longleftrightarrow DMC + NH_3 \tag{1}$$

The macro-kinetic model for the forward and reverse reactions by Arrhenius equations are represented as follows:

$$R = \omega \cdot k_1 \exp(-\frac{Ea_1}{R_g T})C_{MC}C_{Me} - \omega \cdot k_2 \exp(-\frac{Ea_2}{R_g T})C_{DMC}C_{NH_3} \tag{2}$$

Where ω represents the amount of catalyst presented in the column section. k_1 and k_2 represent the Arrhenius frequency factors, and Ea_1 and Ea_2 are activation energy for the forward and reverse reactions, respectively. The values of Arrhenius parameters for the synthesis of DMC by urea and methanol over the solid base catalyst are listed in Table 17.

k_1 (g^{-1}mol^{-1}Ls^{-1})	k_2 (g^{-1}mol^{-1}Ls^{-1})	Ea_1 (J/mol)	Ea_2 (J/mol)
1.104E3	1.464E-3	1.01E5	4.90E4

Table 17. Arrhenius parameters for DMC synthesis catalyzed by solid base catalyst

The system of DMC synthesis process in a CD column mainly involved four components: methanol, DMC, MC and ammonia, as the first step reaction was omitted in the distillation column. The boiling points of the pure components at atmospheric pressure was ranged as follows: methanol (Me) 337.66 K; DMC 363.45 K; MC 450.2 K; ammonia (NH$_3$) 239.72 K, respectively. It could be seen that MC should almost exist in the liquid phase in CD process under high pressure and the reactions would take place in the liquid phase in a CD reaction zone. The system included a binary azeotrope of Me-DMC and the predicted data have been shown in Table 2, with respective boiling points at different pressures. Since the system included a no condenser component of ammonia and a binary azeotropic pair of methanol-DMC, it shows the strong non-ideal properties and the vapor liquid equilibrium was calculated by the EOS + activity method.

5.3 The non-equilibrium model

The non-equilibrium model is schematically shown in Fig.2. This NEQ stage represents a section of packing in a packed column. The heterogeneously catalyzed synthesis of DMC in CD process is treated as pseudo homogenous. Mass transfers at the vapor-liquid interface are usually described via the well-known two-film model. A rigorous model for catalytic distillation processes have been presented by Hegler, Taylor and Krishna. In the present contribution the two-phase non equilibrium model have been developed to investigate the steady state of the DMC synthesis process in catalytic distillation.

The follow assumptions have been made for the non-equilibrium model: (1) the process reached steady state; (2) the first reaction has been omitted as it took place with high yield in the preheater; (3) the reactions occurred entirely in the liquid bulk; (4) the reactions have been considered as pseudo-homogeneous; (5) the pressure in the CD column has been treated as constant.

The model equations composed of material balance, energy balance, mass transfer, energy transfer, phase equilibria, pressure drop equations and summation equations, which had been showed under the follows:

The material balances both for vapor and liquid phase are defined as:

$$V_{j+1}y_{i,j+1} - (1+S_j^V)V_jy_{i,j} + F_j^V z_{i,j}^V - N_{i,j}^V = 0 \tag{3}$$

$$L_{j-1}x_{i,j-1} - (1+S_j^L)L_jx_{i,j} + F_j^L z_{i,j}^L + N_{i,j}^L + R_{i,j}^L = 0 \tag{4}$$

The multi-component mass transfer rates are described by the generalized Maxwell-Stefan equations. The mass transfer equations for liquid phase are described as follow:

$$-\frac{x_i}{R_gT}\nabla_T\mu_i = \sum_{\substack{j=1\\j\neq i}}^{c}\frac{x_jN_i^L - x_iN_j^L}{C_t^L k_{ij}^L a} \tag{5}$$

where μ_i represent the chemical potential, k_{ij}^L is liquid mass transfer coefficient. Only $c-1$ of these equations are independent. The vapor phase mass transfer has a similar relation to the liquid phase.

The energy balances for both vapor and liquid phase are defined as:

$$V_{j+1}H_{j+1}^V - (1+S_j^V)V_jH_j^V + F_j^V H_j^{VF} - e_j^V + Q_j^V = 0 \tag{6}$$

$$L_{j-1}H_{j-1}^L - (1+S_j^L)L_jH_j^L + F_j^L H_j^{LF} + e_j^L + H_j^{LR} + Q_j^L = 0 \tag{7}$$

where the vapor and liquid energy transfer rate is considered as equal. The vapor heat transfer rate is defined as:

$$e^V = -h^V a\frac{\partial T^V}{\partial \eta} + \sum_{i=1}^{C}N_i^V H^V \tag{8}$$

The Vapor-liquid equilibrium occurs at the vapor-liquid interface:

$$y_{i,j}^I - K_{i,j}^I x_{i,j}^I = 0 \tag{9}$$

where the superscript I denotes the equilibrium compositions at the vapor-liquid interface and $K_{i,j}^I$ represents the vapor liquid equilibrium ratio for component i on stage j. And the equilibrium constant is computed by:

$$K_i^I = \frac{P_i^0\gamma_i f_i^0}{Pf_i} \tag{10}$$

The Wilson equations for the liquid phase have been selected to calculate the liquid activity coefficient.

In addition to the above equations, there also have the summation equations for the mole fractions:

$$\sum_{i=1}^{C} x_{i,j} - y_{i,j} = 0 \tag{11}$$

Thermo-physical constants such as density, enthalpy, heat conductivity, viscosity, and surface tension have been calculated based on the correlations suggested by Reid et al. (1987) and by Danbert and Danner (1989). Furthermore, the mass transfer coefficients are computed by the empirical Onda relations.

$$k_{ik}^L = 0.0051(\frac{w^L}{a_w g})^{2/3} \left(\frac{\mu_m^L}{\rho_m^L D_{ik}^L}\right)^{-0.5} \left(\frac{\mu_m^L g}{\rho_m^L}\right)^{1/3} \left(a_t d_p\right)^{0.4} \tag{12}$$

$$k_{ik}^V = \alpha(\frac{w^V}{a_t \mu_m^V})^{0.7} \left(Sc_{ik}^V\right)^{1/3} \left(a_t d_p\right)^{-2} \frac{a_t D_{ik}^V p}{p_{Bm} R_g T} \tag{13}$$

where α is 2.0 for the non-reaction packing of 3.2 mm metal grid ring. The wet area of the packing is estimated using the equations developed by onda et al shown as follow:

$$\frac{a_w}{a_t} = 1 - \exp[-1.45(\frac{w^L}{a_t \mu_m^L})^{0.1} \left(\frac{w^{L2} a_t}{\rho_m^{L2} g}\right)^{-0.05} \left(\frac{w^{L2}}{\rho_m^L \sigma a_t}\right)^{0.2} \left(\sigma_C / \sigma\right)^{0.75}] \tag{14}$$

The effective interfacial area is estimated using the empirical relation developed by Billet:

$$\frac{a}{a_t} = \frac{1.5}{\left(a_t 4\varepsilon/a_t\right)^{0.5}} \left(\frac{u^L 4\varepsilon/a_t}{\mu_m^L / \rho_m^L}\right)^{-0.2} \left(\frac{u^{L2} \rho_m^L 4\varepsilon/a_t}{\sigma_m^L}\right)^{0.75} \left(\frac{u^{L2}}{g 4\varepsilon/a_t}\right)^{-0.45} \tag{15}$$

The mass transfer coefficients for the reaction zone are estimated using the equations developed by Billet, as shown as follow:

$$k_{ik}^L a = 1.13 \frac{a_t^{2/3}}{\left(4\varepsilon/a_t\right)^{0.5}} D_{ik}^{L\,0.5} \left(\frac{g}{\mu^L / \rho^L}\right)^{1/6} \mu_m^{L\,1/3} \frac{a}{a_t} \tag{16}$$

$$k_{ik}^L a = 0.275 \frac{a_t^{3/2}}{\left(4\varepsilon/a_t\right)^{0.5}} D_{ik}^V \frac{1}{\left(\varepsilon - h_L\right)^{0.5}} \left(\frac{\mu_m^V / \rho_m^V}{D_{ik}^V}\right)^{1/3} \left(\frac{u_m^V}{a\mu_m^V / \rho_m^V}\right)^{3/4} \frac{a}{a_t} \tag{17}$$

Heat transfer coefficients are predicted using Chilton-Colburn analogy as follow:

$$h^V = k_{av}^V C_{pm}^V \left(Le^V\right)^{2/3} \text{ for vapor phase}$$

$$h^L = k_{av}^L C_{pm}^L \left(Le^L\right)^{1/2} \text{ for liquid phase.} \tag{18}$$

5.4 The treatment of the reaction for the synthesis of DMC

Commonly, the reaction rates are determined by the concentration of the component, not the volume of the component. And this factor could cause a negative composition of a component during the iteration for the solving of a catalytic distillation model. Consequently, the reaction of a system can be considered as the combination of the positive reactions and the negative reactions.

$$R_{i,j}^L = R_{i,j}^+ + R_{i,j}^- = \sum_{m=1}^{nr}\left(\varepsilon_j \cdot v_{i,m}^+ r_{m,j}^+ - \varepsilon_j \cdot v_{i,m}^- r_{m,j}^-\right) \tag{19}$$

Defined the consumptive coefficient as:

$$E_{i,j}^R = -R_{i,j}^- \big/ x_{i,j} \tag{20}$$

For the condition of x_i equal zero, the consumptive coefficient is set to zero.

5.5 The method of Maxwell-Stefan equations

For the multi-component mass transfer in the catalytic distillation can be considered as the one dimensional mass transfer behavior[13]. And the vapor liquid equilibria is achieved at the vapor liquid interface. It can be noticed that there are no accumulation on the vapor liquid interface and the mass transfer of vapor and liquid are equal to each other.
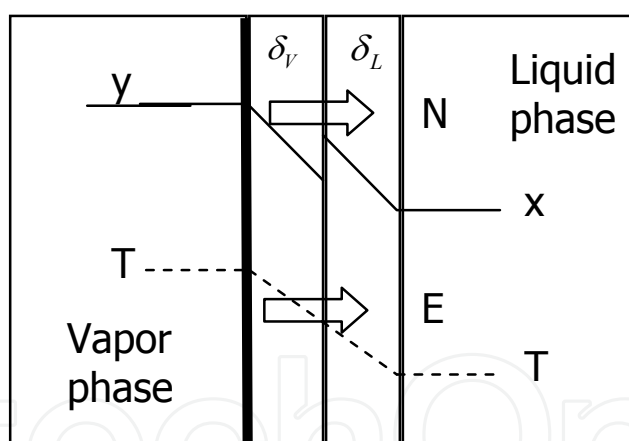
Fig. 2. The multi-components mass transfer

According to the two-film theory, the Maxwell-Stefan equations for vapor and liquid phase are shown as:

$$-\frac{x_i}{RT}\nabla_T \mu_i = \sum_{\substack{j=1 \\ j\neq i}}^{c}\frac{x_j N_i - x_i N_j}{C_t k_{ij}} = \sum_{\substack{j=1 \\ j\neq i}}^{n}\frac{x_j J_i - x_i J_j}{C_t k_{ij}} \tag{21}$$

$$-\frac{y_i}{RT}\nabla_T \mu_i = \sum_{\substack{j=1 \\ j\neq i}}^{c}\frac{y_j N_i - y_i N_j}{C_t k_{ij}} = \sum_{\substack{j=1 \\ j\neq i}}^{n}\frac{y_j J_i - y_i J_j}{C_t k_{ij}} \tag{22}$$

For the liquid mass transfer equations, it could be rearranged by n-1 matrix as:

$$\left(N^L\right) = -C_t^L\left[k^L\right]\frac{\partial x}{\partial \eta} + \left(x\right)N_t^L \tag{23}$$

Where:

$$\left[k^L\right] = \left[R\right]^{-1}\left[\Gamma\right]$$

$$R_{ii} = \frac{x_i}{k_{in}} + \sum_{\substack{k=1 \\ k \neq i}}^{n}\frac{x_k}{k_{ik}} \quad , \quad R_{ij} = -x_i\left(\frac{1}{k_{ij}} - \frac{1}{k_{in}}\right) \tag{24}$$

Γ represent the matrix of Thermal factor for multi-component. The elements of the thermal factor matrix are the partial molar difference of activity coefficient of the component mixture, which could be computed as follow:

$$\Gamma_{ij} = \delta_{ij} + x_i\frac{\partial \ln \gamma_i}{\partial x_j}\bigg|_{\sum x_j = 1} \tag{25}$$

$$i,j = 1,2,3,\cdots,n-1$$

Note: This solution of partial molar difference of activity coefficient was restricted by the summation equation. This should be especially noted.

For the liquid mass transfer equation, it could be written as:

$$\left(J^L\right) = C_t^L\left[k^L\right]\frac{\partial x}{\partial \eta} \tag{26}$$

The mass transfer rates were consistent along the film distance, and the differential equation could be written as:

$$\left(\frac{dx}{d\eta}\right) = \left[\Phi\right]\left(x\right) + \left(\zeta\right) \tag{27}$$

$$\Phi_{ii} = \frac{N_i}{C_t^L k_{in}} + \sum_{\substack{k=1 \\ k \neq i}}^{n}\frac{N_k}{C_t^L k_{ik}} \quad , \quad \Phi_{ij} = -N_i\left(\frac{1}{C_t^L k_{ij}} - \frac{1}{C_t^L k_{in}}\right)$$

$$i,j = 1,2,3,\cdots,n-1$$

There were two boundary conditions as follow.

$$\eta = 0, (bulk), (y) = (y_b)$$

$$\eta = 1, (film), (y) = (y_I) \tag{28}$$

The differential equations could be solved as:

$$\left(x_\eta - x_b\right) = \{\exp([\Phi]\eta) - [I]\} \cdot \{\exp[\Phi] - [I]\}^{-1} \cdot \left(x_I - x_b\right) \tag{29}$$

Additionally, the mass transfer fluxes were expressed as:

$$\left.\frac{d(x)}{\eta}\right|_{\eta=0} = [\Phi] \cdot \{\exp[\Phi] - [I]\}^{-1} \cdot \left(x_I - x_b\right) \tag{30}$$

$$\left(J^L\right) = C_t^L \left[k^L\right][\Phi] \cdot \{\exp[\Phi] - [I]\}^{-1} \cdot \left(x_I - x_b\right) \tag{31}$$

The energy balance should occur on the vapor liquid interface, and these could be written as:

$$\sum_{i=1}^{n} N_i \cdot (\overline{H_i^V} - \overline{H_i^L}) = 0 \tag{32}$$

$$\sum_{i=1}^{n} (J_i + x_i N_t) \cdot (\overline{H_i^V} - \overline{H_i^L}) = 0 \tag{33}$$

$$\beta_{ik} \equiv \delta_{ik} - x_i \Lambda_k$$

$$\Lambda_k = (v_k - v_n) / \sum_{j=1}^{n} v_j x_j \tag{34}$$

As a result, the mass transfer rate could be described as:

$$N_t = -\sum_{i=1}^{n} J_i \cdot (\overline{H_i^V} - \overline{H_i^L}) \bigg/ \sum_{i=1}^{n} y_i \cdot (\overline{H_i^V} - \overline{H_i^L}) \tag{35}$$

$$N^L = c_t^L \left[\beta^V\right] \cdot \left[R^L\right]^{-1} \cdot \left[\Gamma^L\right] \cdot \left[\Xi^V\right] \cdot \left(x^I - x^b\right) \tag{36}$$

Where the high flux correction factor were defined as:

$$[\Xi] = [\Gamma]^{-1} [\Phi] \cdot \left[\exp[\Gamma]^{-1} [\Phi] - [I]\right]^{-1} \tag{37}$$

Similarly, the mass transfer for vapor phase could be described as:

$$N^V = c_t^V \left[\beta^V\right] \cdot \left[R^V\right]^{-1} \cdot \left[\Gamma^V\right] \cdot \left[\Xi^V\right] \cdot \left(y^b - y^I\right) \tag{38}$$

The total mass transfer rates described by vapor phase were showed as:

$$N = c_t^V \left[\beta^V\right] \cdot \left[K_{ov}\right] \cdot \left[\Xi^V\right] \cdot \left(y^b - y^*\right) \tag{39}$$

The solving for these mass transfer equations involved an iterative method and the more mathematic knowledge were needed for the calculation of high flux correction factor, which exponent calculations for a matrix were involved. The computational codes have been developed by the author. Otherwise, these equations were more complicated for the mass transfer in a catalytic distillation system.

Power et al. (1988) found that the high flux correction factor, which is for the calculation of multi-component mass transfer, is not important in distillation and it has been ignored in the calculation for distillation system. In the non-equilibrium stage model of Krishnamurthy and Taylor (1993), the total mass transfer rates are obtained by combining the liquid and vapor mass transfer equations, which the high flux correction factor has been ignored, and multiplying by the interfacial area available for mass transfer. As a result, the total mass transfer rates for the vapor phase described as matrix form are: [14]

$$N_j^L = N_j^V = C_{t,j}^V \left[\beta_j^V \right] \left[K_j^{OV} \right] a_j \left(y_j - y_j^* \right) \tag{40}$$

$$\left[K_j^{OV} \right]^{-1} = \left[K_j^V \right]^{-1} + \frac{C_{t,j}^V}{C_{t,j}^L} \left[K_j^E \right] \left[K_j^L \right]^{-1} \left[\beta_j^L \right]^{-1} \left[\beta_j^V \right] \tag{41}$$

$$\left[K_j^V \right] = \left[\Omega_j^V \right]^{-1}$$

$$\Omega_{ii,j}^V = \frac{y_{i,j}}{k_{iC,j}^V} + \sum_{\substack{l=1 \\ l \neq i}}^{C} \frac{y_{l,j}}{k_{il,j}^V} \quad , \quad \Omega_{ik,j}^V = -y_{i,j} \left(\frac{1}{k_{ik,j}^V} - \frac{1}{k_{iC,j}^V} \right) \tag{42}$$

Where i ,k=1, 2, ···, c-1.

$$\beta_{ik,j}^V = \delta_{ik} - y_{i,j} \left(\Delta H_{k,j}^{Vap} - \Delta H_{n,j}^{Vap} \right) \Big/ \sum_{l=1}^{c} y_{l,j} \Delta H_{l,j}^{Vap} \, , \tag{43}$$

The similar correlation can be described for liquid phase. Where δ is the unit matrix.

5.6 Solving of the non-equilibrium model

By combining the above mentioned equations, the vapor component can be determined by the liquid bulk composition, which described by the matrix form as: [15]

$$Y_j = \left(c_{t,j}^V \left[\beta_j^V \right] \left[K_j^{OV} \right] a_j + (1 + S_j^V) V_j [\delta] \right)^{-1} \left(V_{j+1} Y_{j+1} + F_j^V z_j^V + c_{t,j}^V \left[\beta_j^V \right] \left[K_j^{OV} \right] a_j Y_j^* \right) \tag{44}$$

Defined the single stage vaporizing coefficient:

$$E_{i,j}^V = y_{i,j} \Big/ y_{i,j}^* = y_{i,j} \Big/ K_{i,j}^E x_{i,j} \tag{45}$$

For $x_{i,j} = 0$, $E_{i,j}^V = 1$.

And then we can get a modified tri-diagonal matrix method for solving the non-equilibrium stage model of the catalytic distillation.

$$
\begin{vmatrix}
B_{i1} & C_{i1} & & & & \\
A_{i2} & B_{i2} & C_{i2} & & & \\
 & \cdots & & & & \\
 & & A_{i,j} & B_{i,j} & C_{i,j} & \\
 & & & \cdots & & \\
 & & & & A_{i,n} & B_{i,n}
\end{vmatrix}
\cdot
\begin{vmatrix}
x_{i1} \\
x_{i2} \\
\vdots \\
x_{ij} \\
\vdots \\
x_{in}
\end{vmatrix}
=
\begin{vmatrix}
b_{i1} \\
b_{i2} \\
\vdots \\
b_{ij} \\
\vdots \\
b_{in}
\end{vmatrix}
\tag{46}
$$

$$A_{i,j} = L_{j-1}$$
$$B_{i,j} = -(1 + S_j^V)V_j K_{i,j}^E E_{i,j}^V - (1 + S_j^L)L_j x_{i,j} - E_{i,j}^R$$
$$C_{i,j} = V_{j+1} K_{i,j+1}^E E_{i,j+1}^V$$
$$b_{i,j} = -F_j^V z_{i,j}^V - F_j^L z_{i,j}^L - R_{i,j}^+$$

5.7 The model results

The typical modeling data for the catalytic distillation of DMC synthesis process from urea and methanol over solid base catalyst, which was operated under the pressure of 9 atm. [16-17]

Parameter	Measured	Estimated
Temperature of top (^{o}C)	91.0	94.8
Temperature of reboiler (^{o}C)	165.3	169.1
T in reaction zone (^{o}C)	180	181.1
Material feed (mL/h)	20	20
Methanol feed (mL/h)	60	60
Yield of DMC (%)	45	45
Reflux ratio	4	4
Condenser, mass fraction		
Me	0.768	0.782
DMC	0.052	0.053
MC	0	0
Ammonia	0.18	0.165
Rebloiler, mass fraction		
Me	0.260	0.271
DMC	0	0
MC	0.740	0.729
Ammonia	0	0

Parameter	Measured	Estimated
Product, mass fraction		
Me	0.927	0.927
DMC	0.070	0.070
MC	0	0
Ammonia	0.003	0.003

Table 18. Typical results from experiment and predictions for the synthesis of DMC
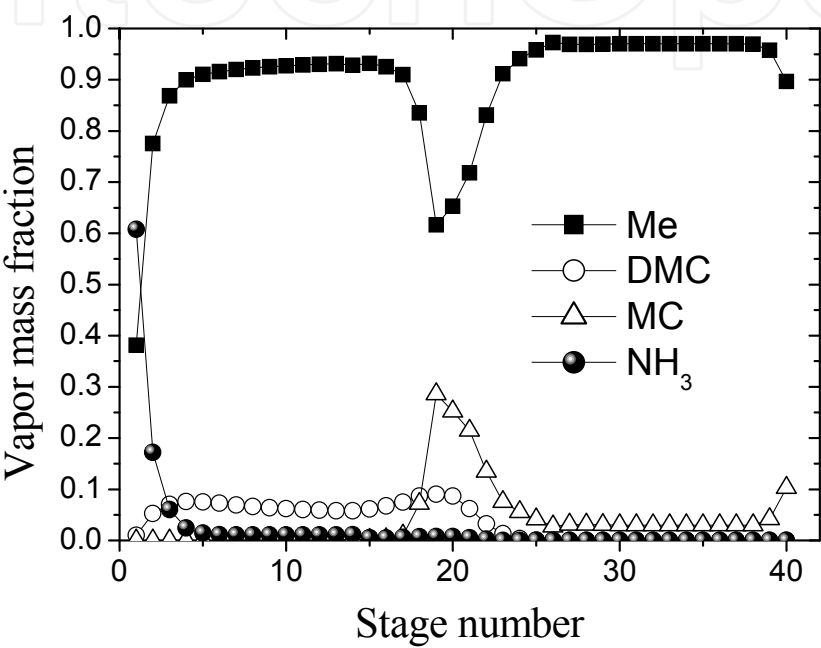
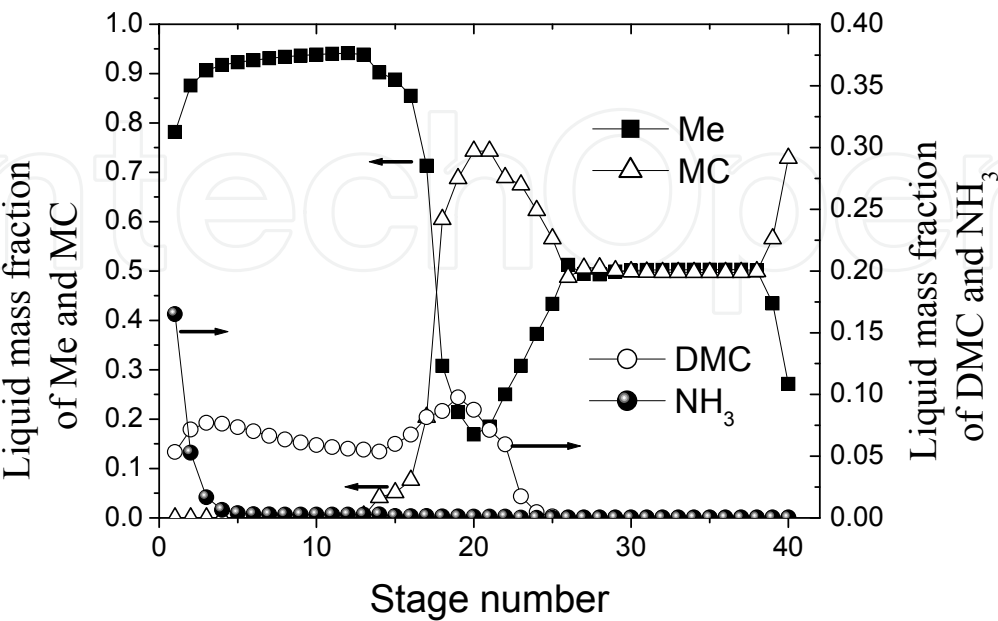Fig. 3. Vapor concentration distribution in distillation column.

Fig. 4. Liquid concentration distribution in distillation column
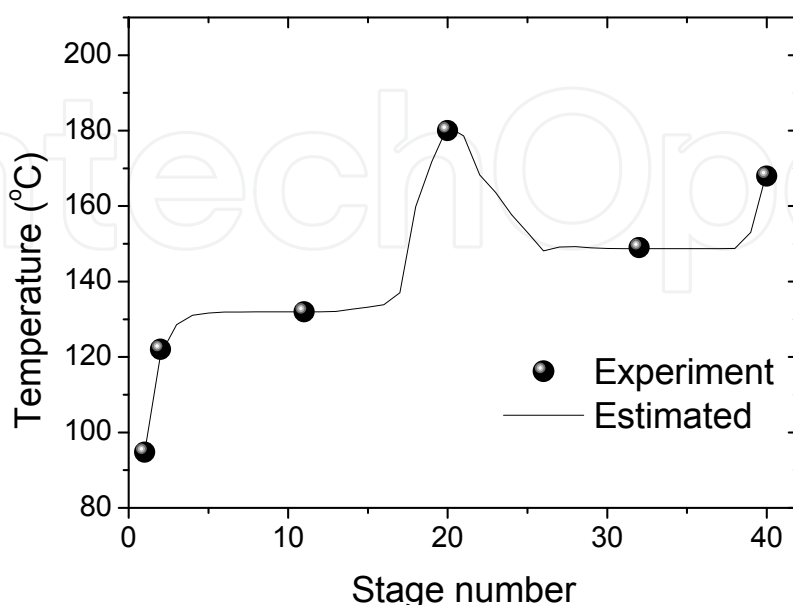
Fig. 5. Temperature distribution in distillation column

6. Separation of the mixture of methanol and DMC

Separation of azeotropic mixtures is a challenge commonly encountered in commodity and fine chemical processes. Many techniques suitable for separation of azeotropic mixtures have been developed recently, such as pressure-swing distillation (PSD), extractive and azeotropic distillation, liquid-liquid extraction, adsorption, prevaporation using membrane, crystallization and some new coupling separation techniques. Despite of the newly developed membrane separation process or adsorption process, it was very important to properly design of the traditional separation of DMC from the reaction mixture using the distillation tower with the existence of the azeotrope of methanol-DMC for large scale of DMC production.

Zhang[18] has developed a process model for atmospheric-pressurized rectification to simulate the separation of DMC and methanol with low concentration DMC, which came from the DMC synthesis through urea methanolysis method. The simulation was carried out based on the Aspen Plus platform with the Wilson liquid activity coefficient model.

Li[4] has given a pressurized-atmospheric separation process for separating the product of DMC from the mixture of methanol and DMC with 30 wt.% of DMC based on the simulation model. They have optimized the operating conditions based on the developed process and the optimized condition: 40 of ideal stages, 29th of feed stage, 7~10 of reflux ratio and 1.3 MPa of pressure for pressurized distillation. However, this process has a drawback of high investment of the equipment and lower stability of operation. Our

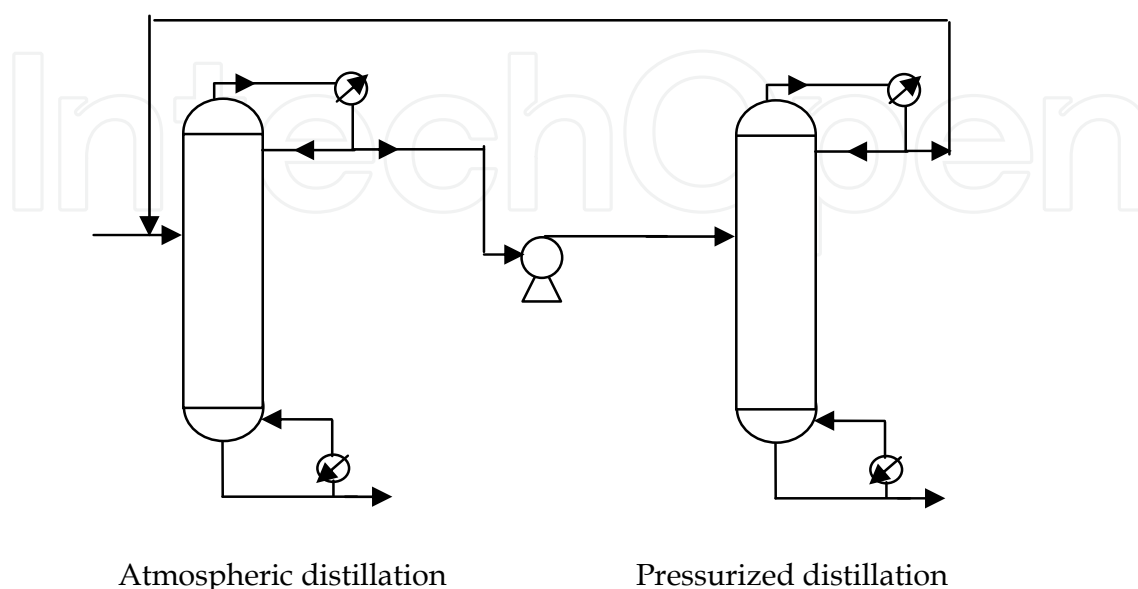Atmospheric distillation   Pressurized distillation

Fig. 6. The schematic diagram of the pressure swing process.

workers, Zhang et al., also developed a novel separation process of atmospheric-pressurized separation process which had the ability to separate the low concentration of DMC for the separation of the mixture with 12 wt.% of DMC base on the 500t/a pilot plant by the simulation model. The sensitive study and the optimization to this process had shown that the reflux ratio for the atmospheric and pressurized distillation had been 3.4 and 1.0 respectively, and 0.65, 0.93 of the distillate to feed ratio for the atmospheric and pressurized distillation. In this process, 99.5wt.% or higher concentration of methanol could be recovered, while the pressurized-atmospheric separation process could only obtained a solution containing 13.3 wt.% of DMC in the recovered methanol stream.

The model simulation and process design for the separation of DMC and methanol has been lettered in many literatures. Much number of the literatures had been presented on the simulation for the DMC synthesis with trans-esterification method, in addition with the detailed research on the catalytic distillation for the DMC synthesis by urea and methanol. However, the simulation work for the other DMC synthesis process had been little reported. Furthermore, the pressure-swing distillation process, the extractive distillation process and the azeotropic distillation process had been developed in the open reported simulative literatures for the product separation of DMC and methanol mixture. Among the derived separation process, the pressure swing distillation process and the extractive distillation process had been considered suitable for the product separation of DMC and methanol mixture.

7. References

[1] Tundo, P.; Selva, M. The Chemistry of Dimethyl Carbonate. Acc. Chem. Res. 2002, 35, 706.

[2] Ono, Y. Dimethyl Carbonate for Environmentally Benign Reactions. Catal. Today 1997, 35, 15.

[3] Rodriguez, J. Canosa, A. Dominguez, J. Tojo. Isobaric vapour–liquid equilibria of dimethyl carbonate with alkanes and cyclohexane at 101.3 kPa. Fluid Phase Equilibria 198 (2002) 95–109.

[4] Rodriguez, J. Canosa, A. Dominguez, J. Tojo. Vapour–liquid equilibria of dimethyl carbonate with linear alcohols and estimation of interaction parameters for the UNIFAC and ASOG method. Fluid Phase Equilibria 201 (2002) 187–201

[5] Ding Wang, Aiguo Xuan, Yuanxin Wua, Zhiguo Yana, Qimei Miao. Study on gas–liquid equilibria with the UNIFAC model for the systems of synthesizing dimethyl carbonate. Fluid Phase Equilibria, 302 (2011) 269 – 273

[6] Wang-Ming Hu, Lv-Ming Shen, Lu-Jun Zhao. Measurement of vapor–liquid equilibrium for binary mixtures of phenol–dimethyl carbonate and phenol–methanol at 101.3 kPa. Fluid Phase Equilibria, 219 (2004) 265–268

[7] Agreda, V. H.; Partin, P. H.; Heise, W. H. High Purity Methyl Acetate via Reactive Distillation. Chem. Eng. Process. 1990, 86, 40.

[8] Pilavachi, P. A.; Schenk, M.; Perez-Cisneros, E.; Gani, R. Modeling and Simulation of Reactive Distillation Operations. Ind. Eng. Chem. Res. 1997, 36, 3188.

[9] Malone, M. F.; Doherty, M. F. Reactive Distillation. Ind. Eng. Chem. Res. 2000, 39, 3953.

[10] Tuchlenski, A.; Beckmann, A.; Reusch, D.; DuKssel, R.; Weidlich, U.; Janowsky, R. Reactive Distillation - Industrial Applications, Process Design & Scale-up. Chem. Eng. Sci. 2001, 56, 387.

[11] Xu, Y.; Zheng, Y.; Ng, F. T. T.; Rempel, G. L. A Three-phase Nonequilibrium Dynamic Model for Catalytic Distillation. Chem. Eng. Sci. 2005, 60, 5637.

[12] Wang Feng, Zhao Ning, Li Junping, et al. Modeling of the Catalytic Distillation Process for the Synthesis of Dimethyl Carbonate by Urea Met hanolysis Method[J]. Ind Eng Chem Res,2007,46(26):8972–8979.

[13] Taylor, R.; Krishna, R. Multicomponent Mass Transfer; John Wiley and Sons: New York, 1993.

[14] Wang Feng, Zhao Ning, LI Jun-ping, Xiao Fu-kui, Wei Wei, Sun Yu-han. Modeling analysis for process operation of synthesis of Dimethyl carbonate. CHEMICAL ENGINEERING(CHINA), 2009, 37(2): 71-74

[15] Wang Feng, Zhao Ning, Li Junping, Xiao Fukui, Wei Wei, Sun Yuhan. Simulation of Catalyst distillation Using Non-Equilibrium model. PETROCHEMICAL TECHNOLOGY, 2007, 36(11): 1128-1133

[16] Wang Feng, Zhao Ning, Li Junping, et al. Non-Equilibrium Model for Catalytic Distillation Process[J].Rront Chem Eng Chin,2008, 2(4): 379-384.

[17] Wang Feng, Zhao Ning, Li Junping, Wu Dudu, Wei Wei, Sun Yuhan. Non-Equilibrium Stage Model for Dimethyl Carbonate Synthesis by Urea Methanolysis in Catalytic Distillation Tower. PETROCHEMICAL TECHNOLOGY, 2008, 37(4): 359-363

[18] Zhang Junliang, Wang Feng, Peng Weicai, Xiao Fukui, Wei Wei, Sun Yuhan. Process Simulation for Separation of Dimethyl Carbonate and Methanol Through Atmospheric-Pressurized Rectification. PETROCHEMICAL TECHNOLOGY, 2010, 39(6): 646-650
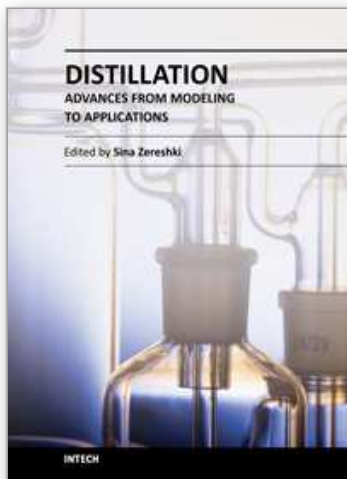
Distillation - Advances from Modeling to Applications

Edited by Dr. Sina Zereshki

Distillation modeling and several applications mostly in food processing field are discussed under three sections in the present book. The provided modeling chapters aimed both the thermodynamic mathematical fundamentals and the simulation of distillation process. The practical experiences and case studies involve mainly the food and beverage industry and odor and aroma extraction. This book could certainly give the interested researchers in distillation field a useful insight.

How to reference

In order to correctly reference this scholarly work, feel free to copy and paste the following:

Feng Wang, Ning Zhao, Fukui Xiao, Wei Wei and Yuhan Sun (2012). The Design and Simulation of the Synthesis of Dimethyl Carbonate and the Product Separation Process Plant, Distillation - Advances from Modeling to Applications, Dr. Sina Zereshki (Ed.), ISBN: 978-953-51-0428-5, InTech, Available from: http://www.intechopen.com/books/distillation-advances-from-modeling-to-applications/the-design-and-simulation-of-the-synthesis-of-dimethyl-carbonate-and-the-product-separation-process-

INTECH
open science | open minds